



Diurnal variations of the optical properties of phytoplankton in a laboratory experiment and their implication for using inherent optical properties to measure biomass

CARINA POULIN,^{1,*} DAVID ANTOINE,² AND YANNICK HUOT¹

¹Géomatique Appliquée, Université de Sherbrooke, 2500, boul. de l'Université, Sherbrooke, J1K 2R1, Canada

²Remote Sensing and Satellite Research Group, Curtin University, Building 301, room 146, GPO Box U1987, Perth, WA 6845, Australia

*carina.poulin@usherbrooke.ca

Abstract: Diurnal variations of phytoplankton size distributions, chlorophyll, carbon and nitrogen content, *in vivo* fluorescence and associated optical absorption and scattering properties were observed in the laboratory to help understand *in situ* and spatial observations. We grew triplicate semi-continuous cultures of *T. pseudonana*, *D. tertiolecta*, *P. tricornutum* and *E. huxleyi* under a sinusoidal light regime. We observed diurnal variations in the particulate absorption (a_p), scattering (b_p), attenuation (c_p), and backscattering coefficients (b_{bp}), which correlate with carbon and Chl concentrations. Relative variations from sunrise of b_{bp} are slightly lower than those of c_p , suggesting that b_{bp} diurnal increases observed in nature are partly caused by phytoplankton. Non-concurrent changes of carbon and Chl-specific backscattering and scattering coefficients and optical cross-sections however indicates that using backscattering to infer scattering or biomass must be done with care.

© 2018 Optical Society of America under the terms of the [OSA Open Access Publishing Agreement](#)

OCIS codes: (010.4450) Oceanic optics; (010.4458) Oceanic scattering; (010.1350) Backscattering; (010.1030) Absorption; (010.0010) Atmospheric and oceanic optics.

References and links

1. C. R. McClain, "A decade of satellite ocean color observations," *Annu. Rev. Mar. Sci.* **1**, 19–42 (2009).
2. J. -K. Choi, Y. J. Park, J. H. Ahn, H. -S. Lim, J. Eom and J. -H. Ryu, "GOFCI, the world's first geostationary ocean color observation satellite, for the monitoring of temporal variability in coastal water turbidity," *J. Geophysical Res.: Oceans* **117**, C9 (2012).
3. R. W. Preisendorfer, *Hydrologic optics. Vol. I. Introduction*. US Department of Commerce, National Oceanic and Atmospheric Administration (Environment Research Laboratory, 1976).
4. R. R. Bidigare, J. H. Morrow, and D. A. Kiefer, "Derivative analysis of spectral absorption by photosynthetic pigments in the western Sargasso Sea," *J. Mar. Res.* **47**, 323–341 (1989).
5. A. Bricaud, A. Morel, and L. Prieur, "Optical efficiency factors of some phytoplankton," *Limnol. Oceanogr.* **28**, 816–832 (1983).
6. A. Morel and A. Bricaud, "Inherent optical properties of algal cells including picoplankton: theoretical and experimental results," *Can. Bull. Fish. Aquat. Sci.* **214**, 521–559 (1986).
7. E. Boss and W. S. Pegau, "Relationship of light scattering at an angle in the backward direction to the backscattering coefficient," *Appl. Opt.* **40**(30), 5503–5507 (2001).
8. M. J. Behrenfeld, E. Boss, D. A. Siegel, and D. M. Shea, "Carbon-based ocean productivity and phytoplankton physiology from space," *Global Biogeochem. Cycles* **19**, 1 (2005).
9. H. R. Gordon and A. Y. Morel, *Remote Assessment of Ocean Color for Interpretation of Satellite Visible Imagery: A Review* (Springer Science & Business Media, 2012).
10. W. D. Gardner, I. D. Walsh, and M. J. Richardson, "Biophysical forcing of particle production and distribution during a spring bloom in the North Atlantic," *Deep Sea Res. Part II Top. Stud. Oceanogr.* **40**, 171–195 (1993).
11. H. Loisel and A. Morel, "Light scattering and chlorophyll concentration in case 1 waters: A reexamination," *Limnol. Oceanogr.* **43**, 847–858 (1998).
12. H. Claustre, A. Morel, M. Babin, C. Cailliau, D. Marie, J.-C. Marty, D. Tailliez, and D. Vaulot, "Variability in particle attenuation and chlorophyll fluorescence in the tropical Pacific: Scales, patterns, and biogeochemical implications," *J. Geophysical Research: Oceans* **104**, 3401–3422 (1999).
13. O. Ulloa, S. Sathyendranath, and T. Platt, "Effect of the particle-size distribution on the backscattering ratio in seawater," *Appl. Opt.* **33**(30), 7070–7077 (1994).

14. A. Morel and S. Maritorena, "Bio-optical properties of oceanic waters: A reappraisal," *J. Geophysical Res.: Oceans* **106**, 7163–7180 (2001).
15. M. S. Twardowski, E. Boss, J. B. Macdonald, W. S. Pegau, A. H. Barnard, and J. R. V. Zaneveld, "A model for estimating bulk refractive index from the optical backscattering ratio and the implications for understanding particle composition in case I and case II waters," *J. Geophysical Res.: Oceans* **106**, 14129–14142 (2001).
16. Y. Huot, A. Morel, M. S. Twardowski, D. Stramski, and R. A. Reynolds, "Particle optical backscattering along a chlorophyll gradient in the upper layer of the eastern South Pacific Ocean," *Biogeosciences Discuss.* **4**, 4571–4604 (2007).
17. D. Vaultot, D. Marie, R. J. Olson, and S. W. Chisholm, "Growth of prochlorococcus, a photosynthetic prokaryote, in the equatorial pacific ocean," *Science* **268**(5216), 1480–1482 (1995).
18. L. Suzuki and C. H. Johnson, "Algae know the time of day: circadian and photoperiodic programs," *J. Phycol.* **37**, 933–942 (2001).
19. F. Bruyant, M. Babin, B. Genty, O. Praslin, M. J. Behrenfeld, H. Claustre, A. Bricaud, L. Garczarek, J. Holtzendorff, and M. Koblizek, "Diel variations in the photosynthetic parameters of Prochlorococcus strain PCC 9511: Combined effects of light and cell cycle," *Limnol. Oceanogr.* **50**, 850–863 (2005).
20. T. G. Owens, P. G. Falkowski, and T. E. Whitledge, "Diel periodicity in cellular chlorophyll content in marine diatoms," *Mar. Biol.* **59**, 71–77 (1980).
21. D. Stramski and R. A. Reynolds, "Diel variations in the optical properties of a marine diatom," *Oceanography (Wash. D.C.)* **38**, 1347 (1993).
22. S. Jacquet, F. Partensky, D. Marie, R. Casotti, and D. Vaultot, "Cell cycle regulation by light in Prochlorococcus strains," *Appl. Environ. Microbiol.* **67**(2), 782–790 (2001).
23. M. D. DuRand, R. E. Green, H. M. Sosik, and R. J. Olson, "Diel variations in optical properties of Micromonas pusilla (prasinophyceae) 1," *J. Phycol.* **38**, 1132–1142 (2002).
24. C. Poulin, F. Bruyant, M.-H. Laprise, A. M. Cockshutt, J. M.-R. Vandenhecke, and Y. Huot, "The impact of light pollution on diel changes in the photophysiology of *Microcystis aeruginosa*," *J. Plankton Res.* **36**, 286–291 (2013).
25. L. W. Harding, B. W. Meeson, B. B. Prézelin, and B. M. Sweeney, "Diel periodicity of photosynthesis in marine phytoplankton," *Mar. Biol.* **61**, 95–105 (1981).
26. H. Claustre, A. Bricaud, M. Babin, F. Bruyant, L. Guillou, F. Le Gall, D. Marie, and F. Partensky, "Diel variations in Prochlorococcus optical properties," *Limnol. Oceanogr.* **47**, 1637–1647 (2002).
27. M. D. DuRand and R. J. Olson, "Diel patterns in optical properties of the chlorophyte *Nannochloris* sp.: Relating individual-cell to bulk measurements," *Limnol. Oceanogr.* **43**, 1107–1118 (1998).
28. N. Ohi, Y. Ishiwata, and S. Taguchi, "Diel patterns in light absorption and absorption efficiency factors of *isochrysis galbana* (prymnesiophyceae) 1," *J. Phycol.* **38**, 730–737 (2002).
29. D. Stramski, A. Shalapyonok, and R. A. Reynolds, "Optical characterization of the oceanic unicellular cyanobacterium *Synechococcus* grown under a day-night cycle in natural irradiance," *J. Geophysical Res.: Oceans* **100**, 13295–13307 (1995).
30. D. A. Siegel, T. D. Dickey, L. Washburn, M. K. Hamilton, and B. G. Mitchell, "Optical determination of particulate abundance and production variations in the oligotrophic ocean," *Deep-Sea Res. A, Oceanogr. Res. Pap.* **36**, 211–222 (1989).
31. J. J. Cullen, M. R. Lewis, C. O. Davis, and R. T. Barber, "Photosynthetic characteristics and estimated growth rates indicate grazing is the proximate control of primary production in the equatorial Pacific," *J. Geophysical Res.: Oceans* **97**, 639–654 (1992).
32. M. D. Durand and R. J. Olson, "Contributions of phytoplankton light scattering and cell concentration changes to diel variations in beam attenuation in the equatorial Pacific from flow cytometric measurements of pico-, ultra- and nanoplankton," *Deep Sea Res. Part II Top. Stud. Oceanogr.* **43**, 891–906 (1996).
33. J. K. Bishop, S. E. Calvert, and M. Y. Soon, "Spatial and temporal variability of POC in the northeast Subarctic Pacific," *Deep Sea Res. Part II Top. Stud. Oceanogr.* **46**, 2699–2733 (1999).
34. W. D. Gardner, J. S. Gundersen, M. J. Richardson, and I. D. Walsh, "The role of seasonal and diel changes in mixed-layer depth on carbon and chlorophyll distributions in the Arabian Sea," *Deep Sea Res. Part II Top. Stud. Oceanogr.* **46**, 1833–1858 (1999).
35. M. J. Behrenfeld and E. Boss, "The beam attenuation to chlorophyll ratio: an optical index of phytoplankton physiology in the surface ocean?" *Deep Sea Res. Part I Oceanogr. Res. Pap.* **50**, 1537–1549 (2003).
36. H. Claustre, Y. Huot, I. Obernosterer, B. Gentili, D. Tailliez, and M. Lewis, "Gross community production and metabolic balance in the South Pacific Gyre, using a non intrusive bio-optical method," *Biogeosciences Discuss.* **4**, 3089–3121 (2007).
37. G. Dall'Olmo, T. K. Westberry, M. J. Behrenfeld, E. Boss, and W. H. Slade, "Significant contribution of large particles to optical backscattering in the open ocean," *Biogeosciences* **6**, 947–967 (2009).
38. M. Stramska and T. D. Dickey, "Short-term variations of the bio-optical properties of the ocean in response to cloud-induced irradiance fluctuations," *J. Geophysical Res.: Oceans* **97**, 5713–5721 (1992).
39. H. Loisel, V. Vantrepotte, K. Norkvist, X. Meriaux, M. Kheireddine, J. Ras, M. Pujo-Pay, Y. Combet, K. Leblanc, and G. Dall'Olmo, "Characterization of the bio-optical anomaly and diurnal variability of particulate matter, as seen from scattering and backscattering coefficients, in ultra-oligotrophic eddies of the Mediterranean Sea," *Biogeosciences* **8**, 3295–3317 (2011).

40. M. Kheireddine and D. Antoine, "Diel variability of the beam attenuation and backscattering coefficients in the northwestern Mediterranean Sea (BOUSSOLE site)," *J. Geophysical Res.: Oceans* **119**, 5465–5482 (2014).
41. R. R. L. Guillard and P. E. Hargraves, "Stichochrysis immobilis is a diatom, not a chrysophyte," *Phycologia* **32**, 234–236 (1993).
42. Z. S. Kolber, O. Prasil, and P. G. Falkowski, "Measurements of variable chlorophyll fluorescence using fast repetition rate techniques: defining methodology and experimental protocols," *Biochim. Biophys. Acta* **1367**(1-3), 88–106 (1998).
43. N. A. Welschmeyer, "Fluorometric analysis of chlorophyll a in the presence of chlorophyll b and pheophytins," *Limnol. Oceanogr.* **39**, 1985–1992 (1994).
44. H. L. MacIntyre and J. J. Cullen, "Using cultures to investigate the physiological ecology of microalgae," *Algal culturing techniques* 287–326 (2005).
45. W. H. Slade, E. Boss, G. DallOlmo, M. R. Langner, J. Loftin, M. J. Behrenfeld, C. Roesler, and T. K. Westberry, "Underway and moored methods for improving accuracy in measurement of spectral particulate absorption and attenuation," *J. Atmos. Ocean. Technol.* **27**, 1733–1746 (2010).
46. A. Morel, "Optical properties of pure water and pure sea water," *Opt. Aspects Oceanography* **1**, 1–24 (1974).
47. T. Oishi, "Significant relationship between the backward scattering coefficient of sea water and the scatterance at 120 degrees," *Appl. Opt.* **29**(31), 4658–4665 (1990).
48. J. M. Sullivan, M. S. Twardowski, J. Ronald, V. Zaneveld, and C. C. Moore, "Measuring optical backscattering in water," *Light Scattering Rev.* **7**, 189–224 (2013).
49. D. Stramski, G. Rosenberg, and L. Legendre, "Photosynthetic and optical properties of the marine chlorophyte *Dunaliella tertiolecta* grown under fluctuating light caused by surface-wave focusing," *Mar. Biol.* **115**, 363–372 (1993).
50. A. Prakash, L. Skoglund, B. Rystad, and A. Jensen, "Growth and cell-size distribution of marine planktonic algae in batch and dialysis cultures," *J. Fisheries Board Canada* **30**, 143–155 (1973).
51. A. Bricaud and A. Morel, "Light attenuation and scattering by phytoplanktonic cells: a theoretical modeling," *Appl. Opt.* **25**(4), 571 (1986).
52. D. Stramski and A. Morel, "Optical properties of photosynthetic picoplankton in different physiological states as affected by growth irradiance," *Deep-Sea Res. A, Oceanogr. Res. Pap.* **37**, 245–266 (1990).
53. S. G. Ackleson, J. J. Cullen, J. Brown, and M. Lesser, "Irradiance-induced variability in light scatter from marine phytoplankton in culture," *J. Plankton Res.* **15**, 737–759 (1993).
54. S. Mas, S. Roy, F. Blouin, B. Mostajir, J. C. Therriault, C. Nozais, and S. Demers, "Diel variations in optical properties of *imantonia rotunda* (haptophyceae) and *thalassiosira pseudonana* (bacillariophyceae) exposed to different irradiance levels(1)," *J. Phycol.* **44**(3), 551–563 (2008).
55. M. Ragni and M. R. d'Alcalà, "Circadian variability in the photobiology of *Phaeodactylum tricornutum*: pigment content," *J. Plankton Res.* **29**, 141–156 (2007).
56. W. M. Balch, D. T. Drapeau, T. L. Cucci, R. D. Vaillancourt, K. A. Kilpatrick, and J. J. Fritz, "Optical backscattering by calcifying algae: Separating the contribution of particulate inorganic and organic carbon fractions," *J. Geophysical Res.: Oceans* **104**, 1541–1558 (1999).
57. A. L. Whitmire, W. S. Pegau, L. Karp-Boss, E. Boss, and T. J. Cowles, "Spectral backscattering properties of marine phytoplankton cultures," *Opt. Express* **18**(14), 15073–15093 (2010).
58. Y.-H. Ahn, A. Bricaud, and A. Morel, "Light backscattering efficiency and related properties of some phytoplankters," *Deep-Sea Res. A, Oceanogr. Res. Pap.* **39**, 1835–1855 (1992).
59. W. Zhou, G. Wang, Z. Sun, W. Cao, Z. Xu, S. Hu, and J. Zhao, "Variations in the optical scattering properties of phytoplankton cultures," *Opt. Express* **20**(10), 11189–11206 (2012).
60. C. Linschooten, J. D. Bleijswijk, P. R. Emburg, J. P. Vrind, E. S. Kempers, P. Westbroek, and E. W. Vrind-de Jong, "Role of the light-dark cycle and medium composition on the production of coccoliths by *emiliania huxleyi* (haptophyceae)," *J. Phycol.* **27**, 82–86 (1991).
61. T. K. Westberry, G. Dall'Olmo, E. Boss, M. J. Behrenfeld, and T. Moutin, "Coherence of particulate beam attenuation and backscattering coefficients in diverse open ocean environments," *Opt. Express* **18**(15), 15419–15425 (2010).
62. D. Antoine, D. A. Siegel, T. Kostadinov, S. Maritorena, N. B. Nelson, B. Gentili, V. Vellucci, and N. Guillocheau, "Variability in optical particle backscattering in contrasting bio-optical oceanic regimes," *Limnol. Oceanogr.* **56**, 955–973 (2011).
63. J. M. Vandennehecke, J. Bastedo, A. M. Cockshutt, D. A. Campbell, and Y. Huot, "Changes in the Rubisco to photosystem ratio dominates photoacclimation across phytoplankton taxa," *Photosynth. Res.* **124**(3), 275–291 (2015).
64. M. Chami, E. Marken, J. J. Stammes, G. Khomenko, and G. Korotaev, "Variability of the relationship between the particulate backscattering coefficient and the volume scattering function measured at fixed angles," *J. Geophysical Res.: Oceans* **111**, C5 (2006).
65. T. Harmel, M. Hieronymi, W. Slade, R. Röttgers, F. Roullier, and M. Chami, "Laboratory experiments for inter-comparison of three volume scattering meters to measure angular scattering properties of hydrosols," *Opt. Express* **24**(2), A234–A256 (2016).
66. H. Tan, T. Oishi, A. Tanaka, and R. Doerffer, "Accurate estimation of the backscattering coefficient by light scattering at two backward angles," *Appl. Opt.* **54**(25), 7718–7733 (2015).

1. Introduction

Considering the vastness of the oceans and the cost and limited coverage of in situ measurements, monitoring global phytoplankton biomass and associated primary production necessitates satellite remote sensing. This has been possible for the past 40 years or so [1] using so-called “ocean color” radiometers on Sun-synchronous satellites (e.g., Sea-Viewing Wide Field-of-View Sensor, SeaWiFs, Moderate Resolution Imaging Spectroradiometer, MODIS). The advent of geostationary ocean color sensors such as GOCE (Geostationary Ocean Color Imager) in 2010, however, provides observations about every hour during daylight for latitudes lower than about 50 degrees [2], which is more than ever realized with ocean color remote sensing. This opens the door to large-scale studies of diel variations of phytoplankton physiology, possibly improving estimation of primary productivity.

Phytoplankton are observable from space through their impact on the inherent optical properties of seawater (IOPs) [3], which in turn determine the apparent optical properties (AOPs), such as the reflectance that is derived from the satellite observations. IOPs can be measured in situ as well as in the laboratory. The two fundamental IOPs are the absorption coefficient (a , m^{-1}) and the volume scattering function (VSF or β , $m^{-1} sr^{-1}$). Integration of the VSF provides the scattering coefficient (b , m^{-1}) when performed over all scattering angles or the backscattering coefficient (b_b , m^{-1}) when only angles greater than 90° are included. The beam attenuation coefficient (c , m^{-1}) is the sum of a and b . These properties are additive, meaning they are the sum of their constituents’ optical properties plus those of water itself.

Biological information can be inferred from other optical properties of phytoplankton. Generally, the absorption coefficient is indicative of pigmentation [4–6] and the scattering coefficient is linked to cell size [7] and carbon content [6, 8–12].

Particulate backscattering can give information on the cell size distribution and the bulk refractive index of particles [13–15], but it is still uncertain whether it is significantly influenced by phytoplankton in situ, although relationships between b_{bp} and chlorophyll (Chl) have been found in case 1 waters [16].

Phytoplankton cellular cycles are dictated by the photoperiod [17]. Many in vitro studies have observed phytoplankton circadian rhythms for cellular division [18, 19], pigments and carbon cellular concentration [20–22], cell size [23], fluorescence [19, 24] and photosynthetic carbon fixation [19, 25]. Diel variations of phytoplankton optical properties have also been studied in the laboratory [19, 23, 26–29]. Notably, a daily increase in intracellular carbon concentration causing an increase in cell size and index of refraction and a nighttime decrease due to cell respiration were observed on *Thalassiosira pseudonana* [21] and *Synechococcus* [29].

Optical properties also show diel variations in the ocean. A diurnal increase of c_p has been observed many times [10, 12, 30–38]. Cullen et al. [31] found that particles and heterotrophs have a non-negligible contribution in diel variations of c_p . While phytoplankton are believed to be contributing to less than 20% of the oceanic particulate organic carbon (POC) [12], they have more significant contribution to the diel variations [36] as the c_p measurement is particularly sensitive to the size range of phytoplankton. b_{bp} also shows a daily increase in the ocean, but the relative daily increase is slightly lower than c_p [39, 40].

The diurnal variations of b_{bp} in cultures have not yet been studied and could give some important information on the factors that influence b_{bp} in the ocean.

The main objective of this study was to describe the diel variations in optical properties of phytoplankton cultures, in view of inferring their response to concurrent changes in phytoplankton characteristics such as cell size distributions, and the chlorophyll, carbon and nitrogen content of cells. The underlying assumption is that a better understanding of these relationships could then be applied later to infer biogeochemical information from optical properties as they can be derived from the numerical inversion of satellite ocean color observations.

2. Materials and methods

The species selected for this work (Table 1) are all in the nanoplankton size range and were chosen for their different shapes and pigment compositions, with anticipated impact on their optical properties.

Table 1. Description of the species chosen for the experiments. Numerical values are given as mean \pm standard deviation.

Species	<i>Thalassiosira pseudonana</i> (CCMP 1335)	<i>Dunaliella tertiolecta</i> (CCMP 1320)	<i>Phaeodactylum tricornutum</i> (CPCC 162)	<i>Emiliania huxleyi</i> (CCMP 371)
Taxonomic group	Diatom	Chlorophyte	Diatom	Haptophyte (coccolithophore)
Equivalent spherical diameter (μm)	4.4 ± 0.1	6.0 ± 0.4	4.3 ± 0.1	4.4 ± 0.2
Shape	Cylindrical (centric symmetry) 	Ovoid 	Pennate and oval 	Spherical (covered with coccoliths) 
Chl in cultures ($\mu\text{g}\cdot\text{L}^{-1}$)	150 ± 40	130 ± 40	130 ± 50	80 ± 20
POC in cultures ($\text{g}\cdot\text{m}^{-3}$)	5 ± 2	4 ± 2	3 ± 2	3 ± 1
Values in the containers used for IOP measurements				
Dilution factor for IOPs	37 ± 1	43 ± 2	43 ± 2	110 ± 20
$b_{\text{pp}} 650$ (m^{-1})	0.0010 ± 0.0004	0.0007 ± 0.0001	0.0005 ± 0.0002	0.005 ± 0.002
$a_{\text{p}} 677$ (m^{-1})	0.04 ± 0.01	0.03 ± 0.01	0.03 ± 0.01	0.01 ± 0.005
$b_{\text{p}} 550$ (m^{-1})	0.9 ± 0.3	0.25 ± 0.06	0.3 ± 0.1	0.4 ± 0.2

Two identical experiments with two species each were conducted. Algae were grown in triplicates at 25 °C in 4 litres of L1 medium [41] (or L1 with nutrients diluted 12 times and without silica to allow *E. huxleyi*'s lith production) for at least 10 generations in semi-continuous cultures, diluted once a day, to reach approximately 100 $\mu\text{g}\cdot\text{L}^{-1}$ of chlorophyll a the following day. The biomass was kept near that maximum value to avoid carbon limitation. Eight fluorescent tubes (Philips #147454 F54T5/865/HO/ALTO, Netherlands) whose spectra were modified towards that of sunlight using “Special Lavender” filter (LEE #137 LEE Filters, United Kingdom) provided growth irradiance. Irradiance was computer-controlled to follow a sinusoidal 12h:12h light:dark cycle with a maximum of 400 $\mu\text{mol photons m}^{-2} \text{s}^{-1}$ outside the vessels at 12:00. These irradiance values are higher than those generally used in culture studies, but reflect more closely those encountered those observed in the surface mixed layer.

The sampling was conducted over one day starting one hour before sunrise and ending one hour after sunset. The analyses performed on the samples are described below.

Variable fluorescence was measured after 30 min of dark-acclimation using a 3500 Fluorometer (Photon Systems Instruments, Czech Republic) with a 630 nm LED as the excitation source. Emission was measured through a high-pass 690 nm filter (RG695 filter, Schott, USA) and a 730 nm interference low-pass filter. The results were normalized to rhodamine dye to account for potential instrument drift and culture medium was used for blanks (fluorescence values were the same as the culture filtrate). Fluorescence was measured every microsecond during an 80 μ s, 34 000 μ mol photons $m^2 s^{-1}$ flash providing an induction curve. The F_o and F_m parameters, representing the minimum and maximum values of the fluorescence transient and the absorption cross-section of photosystem II at 630 nm ($\sigma_{PSII}[630]$, angstrom 2 photon $^{-1}$), were obtained by fitting a fluorescence induction model [42] to the data. F_v is calculated as difference between F_m and F_o . We derived the maximum quantum yield of charge separation at photosystem II by computing F_v / F_m .

Chlorophyll a (Chl) concentrations ($\mu\text{g}\cdot\text{L}^{-1}$) were determined by fluorometry using the non-acidification method [43]. Chl from injected 0.2 mL samples was extracted in 2 mL of a 3/2 (v/v) acetone 90%/DMSO solution for 15 min [44]. Afterwards, fluorescence was measured using a Trilogy fluorometer (Turner Designs, USA) fitted with a Chl Non-Acidification Module (Turner Designs, USA) and previously calibrated with a chlorophyll standard.

Cell counts and diameters were measured using a Multisizer 4 Coulter Counter (Beckman Coulter, USA) equipped with a 100 μm aperture tube and calibrated with 5 μm polystyrene beads. Cultures were diluted approximately 100 times (depending on the species) with a twice-filtered 35% NaCl Milli-Q solution before counting.

For carbon (C, $\text{g}\cdot\text{L}^{-1}$) and nitrogen (N, $\text{g}\cdot\text{L}^{-1}$) concentrations, 25 mm GF75 Glass Fiber filters (Advantec, USA) and 7 mL borosilicate vials were pre-cremated, covered with aluminum foil, at 400 °C for 4 hours to remove any trace of carbon. Then 100 mL culture samples were filtered on the prepared filters and placed in the prepared vials, covered with foil, and left to dry in an oven at 60 °C for a minimum of 8 hours. The vials were then placed in a glass desiccator where the desiccant was replaced by fuming 37% V/V HCL overnight for decarbonation. Vials and filters were returned to dry in the oven and then stored in cremated aluminum envelopes in vacuum-sealed bags until analysis. Filters were then placed in tin capsules and analyzed in a Fisons - EA-1108 CHNS-O Element Analyzer (Thermo Scientific, USA).

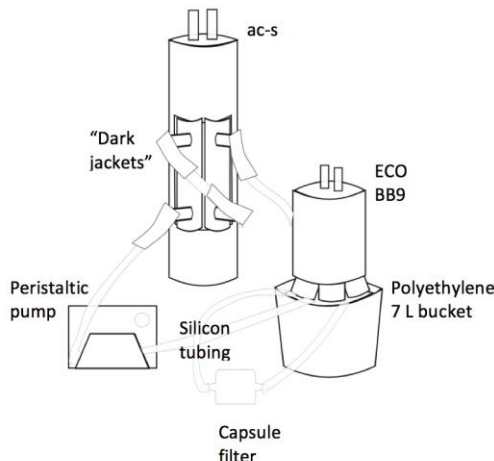


Fig. 1. Experimental setup for the optical instruments made up of a 7 L bucket, an ac-s and an ECO BB9 connected by silicone tubing and a peristaltic pump. A recirculation loop with a 0.2 μm capsule filter was used for filtration between sampling time-points.

Optical measurements were done every two hours with the setup illustrated in Fig. 1. A 7-liter black polyethylene resin plastic (Miller Manufacturing, USA) bucket was filled with twice-filtered (0.2 μm Polycap capsule filter, Watman, USA) salt water. Silicone tubing ran between the bucket, a peristaltic pump and an ac-s spectrophotometer (Wet Labs, USA) and returned to the bucket. Dark jackets were installed on the ac-s tubing to prevent light contamination in the instrument. We installed a parallel network with tubing and a 0.2 μm filter Polycap capsule filter (Watman, USA) for filtrations between samplings. An ECO BB9 backscattering meter (Wet Labs, USA, wavelengths: 407, 439, 485, 507, 527, 594, 651, 715, 878 nm) was placed over the bucket, heads in the water, facing down. We tested that the sides of the bucket did not influence the ECO BB9 by checking stability of measurements while moving the instrument around (with filtered water and in the presence of algae). The calibrations were done with polystyrene beads (0.1 μm , NIST, USA) at the Harbor Branch Oceanographic Institute (USA) 7 months before and 5 months after the experiments. We interpolated the two calibration slopes and darks values to obtain the calibration values for our experiments. A few days after the measurement, using the same polyethylene bucket, ECO BB9 measurements on different concentrations of beads were made to validate the calibration slopes exceeding the range of the measurements for phytoplankton. Our calibration was within 0.3-9% of the interpolated factory calibration. The ac-s calibration stability was verified with air and by pumping Milli-Q (Millipore, USA) using the same setup before and after the experiment. Data processing for the ac-s included interpolation of absorption (a) onto attenuation (c) and a temperature-salinity correction from Slade et al. [45].

We poured a volume of the culture sample varying between 50 mL and 200 mL (depending on the scattering of the cultures during previous tests) in the 7 L bucket and lightly but thoroughly mixed the contents and removed any bubbles on the heads of the ECO BB9 by wiping carefully with a squeegee before measuring simultaneously with the ac-s and the ECO BB9. We obtained the total volume scattering function at 124° from the instrument counts using the interpolated calibration values and subtracted the volume scattering function of water of Morel [46] to obtain the volume scattering function of particles (β_p , m^{-1}) at 124°. The backscattering coefficient (b_b , m^{-1}) can be derived by integrating measurements of the volume scattering function (β) over the backward scattering angles, when such measurements are feasible. Here we only measured $\beta_p(124^\circ)$, and we have used the (χ) factor of Oishi [47]. Therefore, the particulate backscattering coefficient (b_{bp} , m^{-1}) was calculated as:

$$b_{bp} = 2\pi\chi\beta_p(124^\circ) \quad (1)$$

where we used 1.076 [48] for the proportionality constant χ .

While the bucket content was filtered between each bi-hourly sampling to return to blank values, this was not done between each sample. Therefore, for each sample, the particulate absorption coefficient (a_p , m^{-1}), the beam attenuation coefficient (c_p , m^{-1}) and b_{bp} of the preceding sample was subtracted to obtain the particulate coefficients of the measured sample.

We calculated ratios to gain more information from our measurements. Carbon per chlorophyll (C/Chl, g/g) and carbon per nitrogen (C/N, g/g) were studied, along with carbon and chlorophyll per cell (pg-cell^{-1}). We also calculated the mass specific IOPs including the chlorophyll-specific absorption coefficient (a_p^{Chl} , $\text{m}^2 \text{mg}^{-1}$), beam attenuation coefficient (a_p^{Chl} , $\text{m}^2 \text{mg}^{-1}$) and backscattering coefficient b_{bp}^{Chl} ($\text{m}^2 \text{mg}^{-1}$) and the carbon-specific beam attenuation coefficient (c_p^C , $\text{m}^2 \text{g}^{-1}$) and backscattering coefficient b_{bp}^C ($\text{m}^2 \text{mg}^{-1}$). Absorption, scattering, attenuation and backscattering per cell were calculated to obtain the cross-sections (σ_a , σ_b , σ_c , σ_{bb} , $\text{m}^2 \text{cell}^{-1}$).

Percent change from sunrise at time t was calculated as:

$$\Delta b_p(t) = 100 \left[\frac{b_p(t)}{b_p(0)} - 1 \right]. \quad (2)$$

3. Results and discussion

3.1 Biological measurements

Growth rates were stable at least the last 5 days before the sampling day: $1.4 \pm 0.07 \text{ d}^{-1}$ for *T. pseudonana*, $0.85 \pm 0.04 \text{ d}^{-1}$ for *D. tertiolecta*, $1.08 \pm 0.06 \text{ d}^{-1}$ for *P. tricornutum* and $0.64 \pm 0.07 \text{ d}^{-1}$ for *E. huxleyi*. The maximum quantum yield of charge separation at photosystem II (F_v/F_m) varied between 0.42 and 0.61 for all species and showed diel variations, with higher values at the beginning and end of the lit period [Fig. 2] as observed previously on other species [19, 24]. There was a sudden drop in illumination at 20:00 due to a problem in the code managing the lighting system that was found during the analysis of the results. That sharp decrease is not quantitatively important because the cultures were still exposed to a sinusoidal light regime for most of the day and night. A similar sharp decrease in illumination has incidentally also happened in Stramski and Reynolds [21], where it was due to a wall hiding natural sunlight.

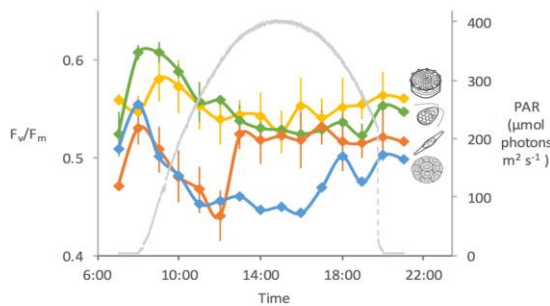


Fig. 2. Diurnal variations of the mean quantum yield of photosynthesis (F_v/F_m) and PAR (gray dashed line, $\mu\text{mol photons m}^{-2} \text{ s}^{-1}$) for the four species: *T. pseudonana* (yellow), *D. tertiolecta* (green), *P. tricornutum* (orange) and *E. huxleyi* (blue). The same color-coding is used throughout the paper. Spline curve fits were added as a visual aid.

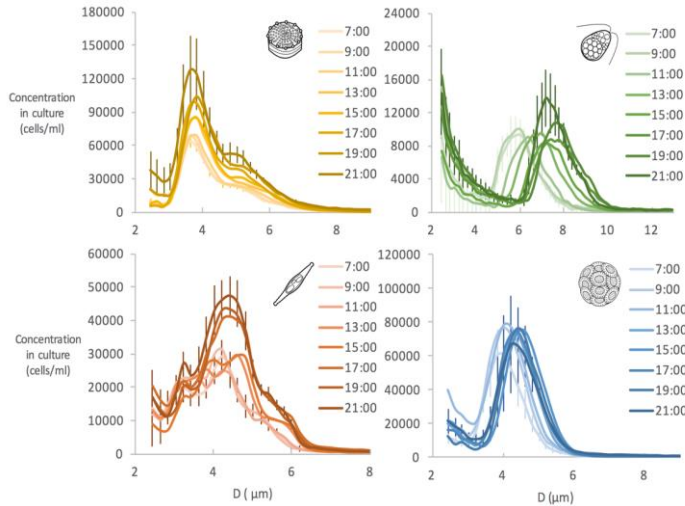


Fig. 3. Diurnal variations of the mean cell size distributions in the cultures, measured with the Coulter Counter, and for the times indicated. Standard deviations (error bars) were added to the 7:00 and 21:00 curves.

Cell size distributions varied during the day. These changes were mostly due to changes in cell concentrations for the diatoms and while changes were mainly in cell diameters for *D.*

tertiolecta and to a lesser degree for *E. huxleyi* [Fig. 3]. The shapes of the distributions are coherent with literature [21, 49–51]. Diameters are presented in terms of equivalent spherical diameters. This is particularly important for *P. tricornutum* which has a length to width ratio of approximately 5. Mean cell diameters (D , μm) generally increased by about 10% (20% for *D. tertiolecta*) after sunrise and plateaued at the end of the lit period [Fig. 4]. This was also observed by Stramski and Reynolds [21] on *T. pseudonana*, Durand and Olson [27] for a chlorophyte and DuRand et al. [23] for a prasinophyte. That increase is likely related to the cell cycle. A sudden increase in cell numbers was observed for *P. tricornutum* at 15:00, possibly due to synchronized cell division, as the mean cell diameter showed a decrease at 17:00. Intracellular carbon concentration (C , $\text{pg}\cdot\text{cell}^{-1}$) increased for all species, while the chlorophyll a concentration (Chl , $\text{pg}\cdot\text{cell}^{-1}$) also increased with a maximum in the late afternoon for diatoms, was stable for *D. tertiolecta* and decreased in the morning, followed by an increase for *E. huxleyi*. A daytime increase is present for C/Chl and C per nitrogen (C/N) (g/g) ratio. The values and shapes of diurnal variations for *T. pseudonana* are similar to the results of Stramski and Reynolds [21].

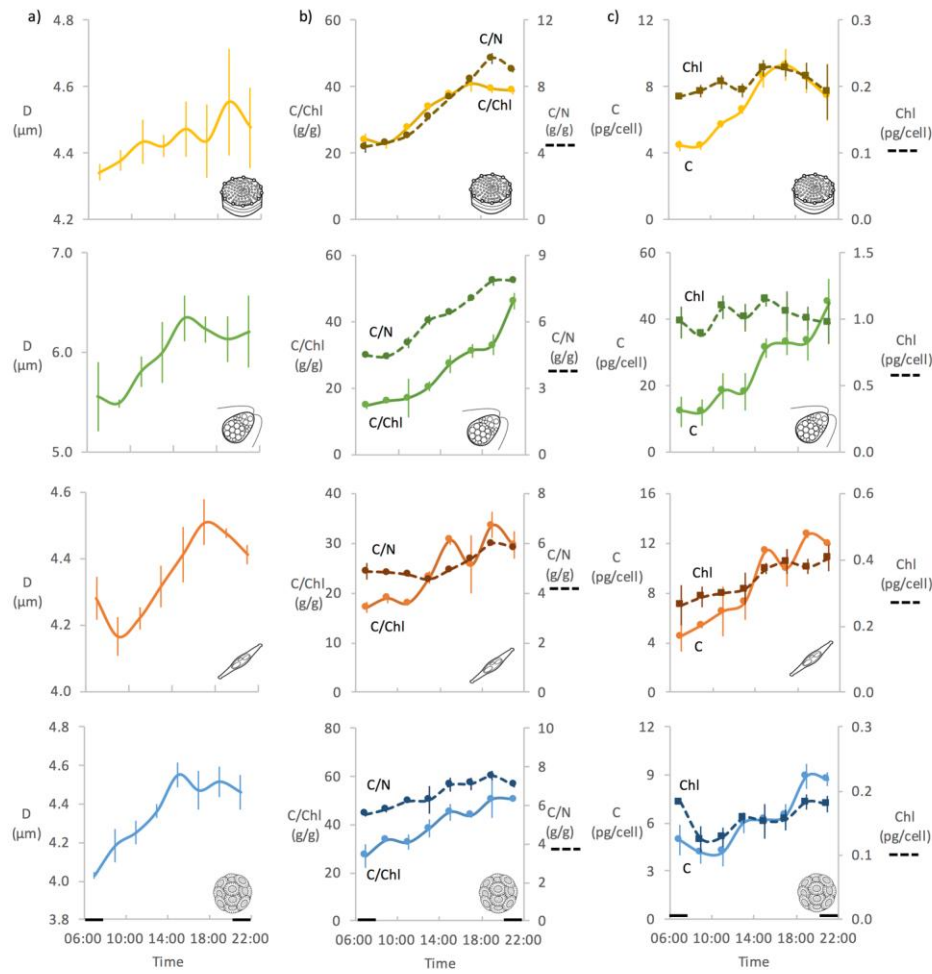


Fig. 4. Diurnal variations of the mean and standard deviations (error bars) of a) cell diameter, b) C/Chl (g/g , solid line) and C/N (g/g , dashed line) and c) intracellular C ($\text{pg}\cdot\text{cell}^{-1}$, solid line) and Chl ($\text{pg}\cdot\text{cell}^{-1}$, dashed line). Spline curve fits were added as a visual aid. Dark bars on x axis represent the dark period of the day. Results from top to bottom are for: *T. pseudonana*, *D. tertiolecta*, *P. tricornutum* and *E. huxleyi*.

3.2 Optical properties

Absorption values were likely slightly contaminated by light passing through the dark jackets installed on the tube attached to the absorption tube of the ac-s in our setup. The movement of these jackets caused results to appear noisy, mostly in the blue wavelengths (up to about 450 nm, see Fig. 5(a)). Averages over about 1 minute show coherent absorption spectra for the other wavelengths, while the shorter wavelengths show significant changes in shape with sampling time that are likely originating from light leaks. We grayed out the shorter wavelengths of a_p and b_p for this reason, although the impact on b_p is very small.

The spectral shapes of a_p , b_p and c_p [Fig. 5] did not vary much throughout the day for all species, except for *T. pseudonana* and *D. tertiolecta*, whose b_p and c_p spectra showed a significant reddening of the spectra with time of day. Values of a_p increased during the day for all species. b_p and c_p [Fig. 6] increased during the day for most species, except for *E. huxleyi* for which there was a plateau from 11:00. These observations are consistent with the observed increases in c_p of nanoplankton in nature that have been observed by Durand and Olson [32].

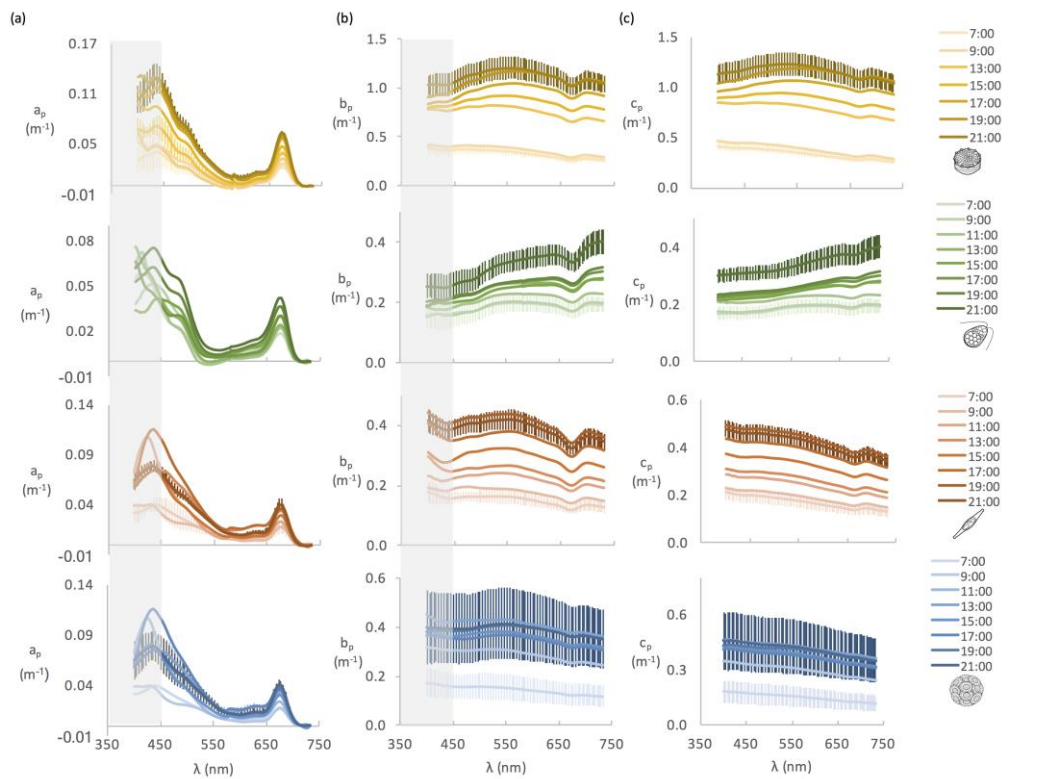


Fig. 5. Diurnal variations of a) particulate absorption coefficient (a_p , m^{-1}), b) particulate scattering coefficient (b_p , m^{-1}) and, c) particulate beam attenuation coefficient (c_p , m^{-1}) at different times of the day (see legend). The standard deviations (error bars) are only displayed for 7:00 and 21:00 when available. Results from top to bottom are for: *T. pseudonana*, *D. tertiolecta*, *P. tricornutum* and *E. huxleyi*.

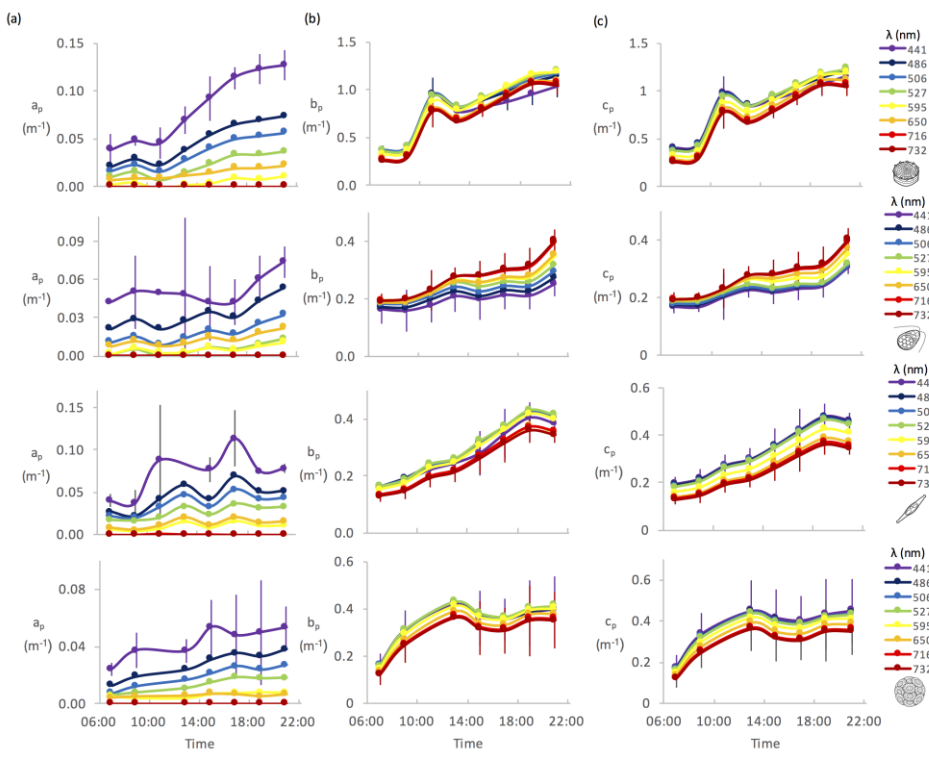


Fig. 6. Diurnal variations of the mean a) particulate absorption coefficient, b) particulate scattering coefficient, c) particulate beam attenuation coefficient for the wavelengths indicated. The standard deviations (error bars) are only displayed for 441 and 732 nm. Results from top to bottom are for: *T. pseudonana*, *D. tertiolecta*, *P. tricornutum* and *E. huxleyi*. Spline curve fits were added as a visual aid.

No diurnal directional changes were observed for the a_p^{Chl} values as error bar overlap for most measurements [Fig. 7(a)], indicating that diurnal variations of a_p are linked to an increase in pigments concentration in the culture with growth, as expected [21, 23, 29]. The c_p^{Chl} has shown some variability and approximately doubled for *T. pseudonana* and *E. huxleyi* [Fig. 7(b)] during the day, and remained more stable than c_p^C , except for *T. pseudonana*. The mean c_p^{Chl} and c_p^C obtained in our experiment for *T. pseudonana* ($\lambda = 673$ and 600 nm respectively) are comparable to the results published by Stramski and Reynolds [21]. c_p^C [Fig. 7(c)] showed an average of $3.9 \pm 1.5 \text{ m}^2 \text{ g}^{-1}$ *D. tertiolecta*. Its value decreased by approximately 66% during the day. This contrasts with the observations of Durand and Olson [27] on *Nannochloris*, where they observed an increase of up to 25% during the day and by Durand et al. [23] on another chlorophyceae species, *Micromonas pusilla*, where an increase of 30% with an average of $2.9 \text{ m}^2 \text{ g}^{-1}$ was noted. *P. tricornutum* showed an average of $3.76 \pm 0.78 \text{ m}^2 \text{ g}^{-1}$ with a morning increase, but an overall decrease of 33% for the day. *E. huxleyi*'s c_p^C had an average of $10.0 \pm 1.5 \text{ m}^2 \text{ g}^{-1}$ and remained mostly constant with a 20% morning increase followed by an equivalent decrease. A similar pattern was observed for *T. pseudonana* with an average of $4.94 \pm 0.52 \text{ m}^2 \text{ g}^{-1}$. Stramski and Reynolds [21] noted an absence of a clear diel pattern for c_p^C for *T. pseudonana* and an average of $3.81 \text{ m}^2 \text{ g}^{-1}$ for their entire diel experiment. They also noted that c_p^C at 660 nm almost doubled during the day for *Synechococcus* [29]. Our results together with those of Durand and Olson [27], Stramski and Reynolds and Stramski et al. [21, 29] indicate that there can be significant diurnal variations in c_p^C and that clear differences occur between species. This has important implications for estimating primary productivity, where c_p^C has been assumed to be constant

and close to $3.92 \text{ m}^2 \text{ g}^{-1}$ [30], which is likely an oversimplification (e.g., Cullen et al. [31]). We also observed that the interspecific variability related to cell size was greater than the diel variability, as shown by Durand et al. [23]. Our species were larger than those presented in Durand et al. [23] from other studies [21, 27, 29, 52], and the relationship between c_p^C and the effective cell diameter (as calculated in [21, 23, 27, 29]) can be fitted by logarithmic function of effective diameter [Fig. 8]. *E. huxleyi* is a clear outlier to this function, however, likely due to the very refractive calcite liths that cover the cells and the fact that our decarbonation of the POC samples removed these calcite shells and therefore only the organic carbon was measured, thus increasing their c_p^C .

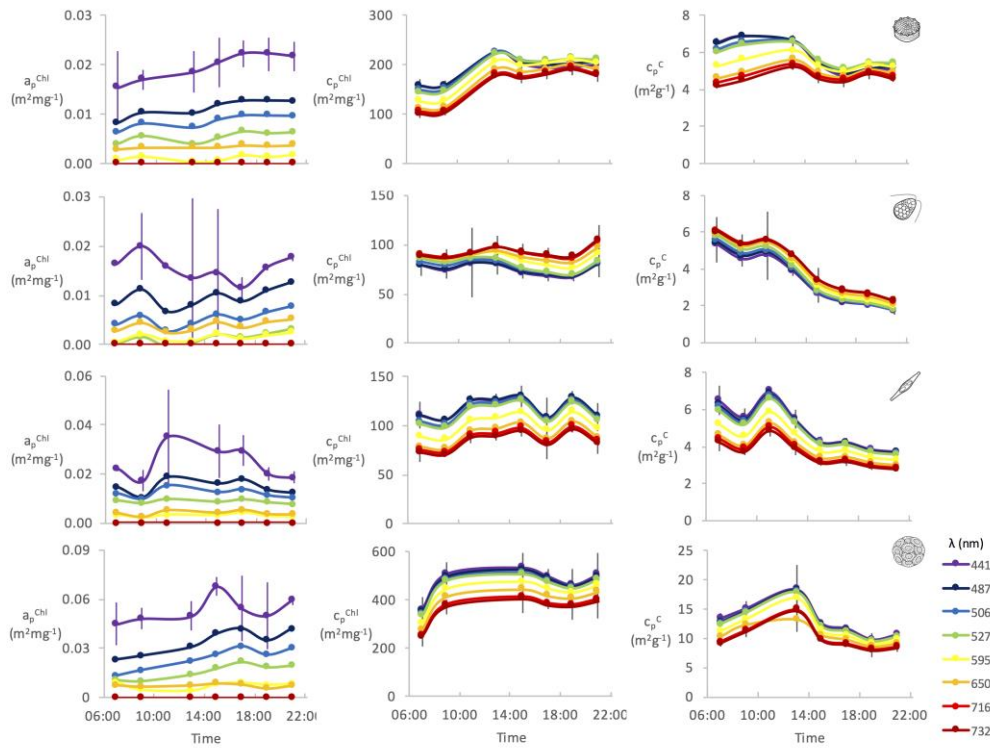


Fig. 7. Diurnal variations of the mean spectral a) chlorophyll-specific particulate absorption coefficient (a_p^{Chl} , $\text{m}^2 \text{ mg}^{-1}$), b) chlorophyll specific particulate beam attenuation coefficient (c_p^{Chl} , $\text{m}^2 \text{ mg}^{-1}$), c) carbon specific particulate beam attenuation coefficient (c_p^C , $\text{m}^2 \text{ g}^{-1}$) for the wavelengths indicated. The standard deviations (error bars) are only displayed for 441 and 732 nm when available. Results from top to bottom are for: *T. pseudonana*, *D. tertiolecta*, *P. tricornutum* and *E. huxleyi*. Spline curve fits were added as a visual aid.

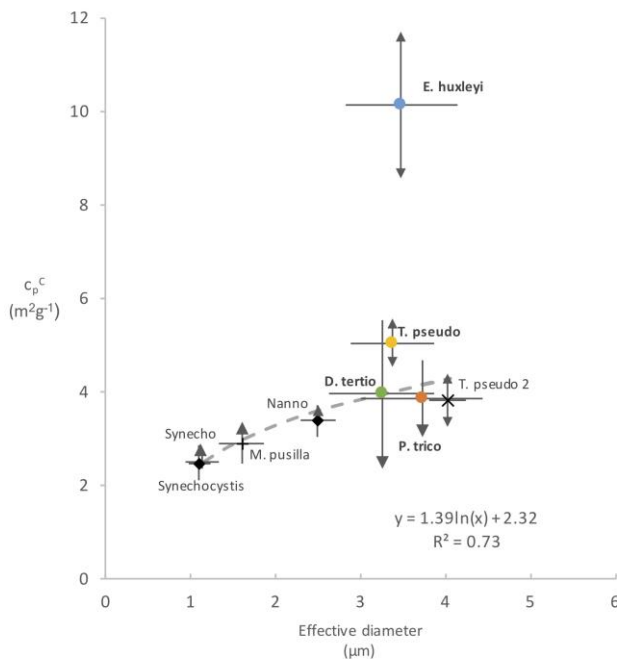


Fig. 8. Relationship between the carbon-specific beam attenuation coefficient ($c_p^C \text{ m}^2 \text{ g}^{-1}$), and effective cell diameter (μm) for nine phytoplankton species, including the four studied in this paper (colored symbols), plus *Synechococcus* (Stramski et al., 1995) [27], *Synechocystis* (Stramski and Morel, 1990) [49], *Micromonas pusilla* [21], (Durand et al., 2002), *Nannochloris* sp. (Durand and Olson, 1998) [25] and *Thalassiosira pseudonana* 2 (Stramski and Reynolds, 1993) [19]. For each point the mean and standard deviations (error bars) over the diel cycle is shown with an arrow indicating direction of the change for c_p^C , except for *Synechocystis* for which the mean of seven different irradiances is shown. c_p^C is at 550 nm except for *Synechocystis* (660 nm).

Spectral shapes of absorption, scattering and attenuation cross-sections (σ_a , σ_b and σ_c , $\text{m}^2 \text{cell}^{-1}$) [Fig. 9] were consistent during the day for *P. tricornutum* and *E. huxleyi*. The spectral shapes of σ_b and σ_c for *T. pseudonana* and *D. tertiolecta* showed a daily increase of the red compared to the blue part of the spectrum, as was seen in b_p and c_p [Fig. 5]. The values were similar to Stramski and Reynolds' [21] for *T. pseudonana*, though they did not observe the same shift in shape that we have.

Values of σ_a showed an increase, especially in the shorter wavelengths, only for *T. pseudonana* as seen by Stramski and Reynolds' [21], Ackleson et al. [53] and Mas et al. [54]. Ragni and Ribera d'Alcalà [55] had observed clearer diurnal variations for *P. tricornutum*, but similar values. σ_b and σ_c showed clear diurnal increases for the diatoms only (*T. pseudonana* and *P. Tricornutum*) [Fig. 9]. The measurements for *P. tricornutum* and *D. tertiolecta* also had a relatively large amount of variation, as shown by the error bars, that likely caused the appearance of bumps in the measurements. This increase indicates that b_p and c_p 's diurnal increases are not only attributable to cell numbers. Diurnal variations and values for *T. pseudonana* were similar to Stramski and Reynolds' [21] and to Durand and Olson [27] on a chlorophyte, for *D. tertiolecta* and Ackleson et al. [53] for *E. huxleyi*. It is worth noting that we included the entire particle size distribution to calculate the cross-sections, so it represents all the particles present in the optical and Coulter Counter measurements, possibly including some non-phytoplanktonic cells.

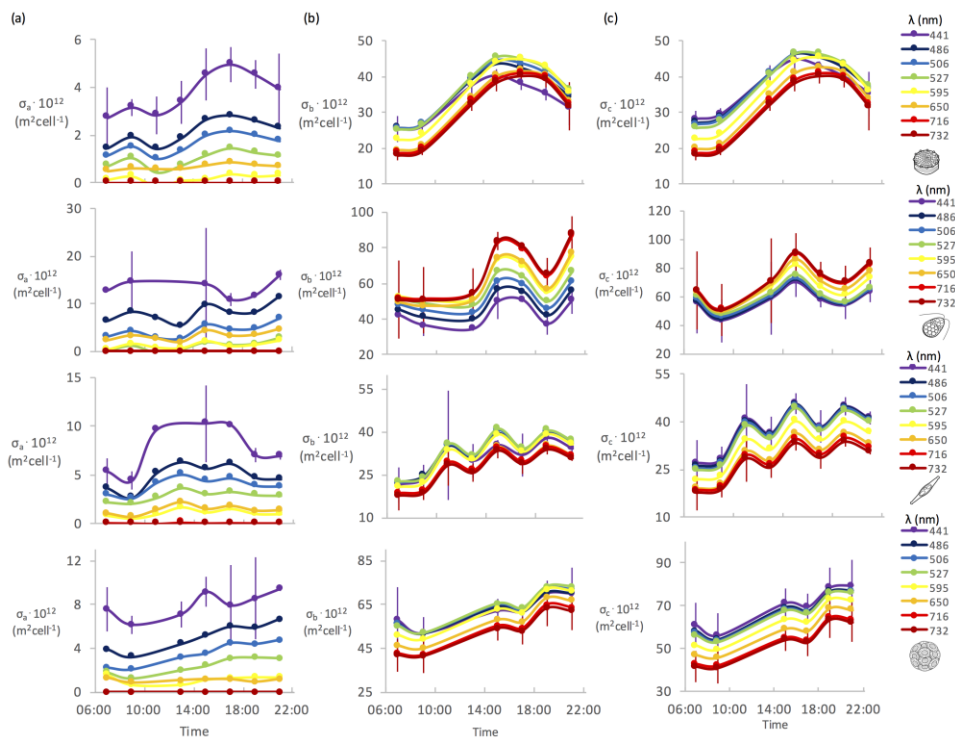


Fig. 9. Diurnal variations of the mean a) particulate absorption cross-section (σ_a , $m^2 \text{ cell}^{-1}$), b) particulate scattering cross-section (σ_b , $m^2 \text{ cell}^{-1}$), c) particulate attenuation cross-section (σ_c , $m^2 \text{ cell}^{-1}$) for and the wavelengths indicated in the legend. The standard deviations (error bars) are only displayed for 441 and 732 nm when available. Results from top to bottom are for: *T. pseudonana*, *D. tertiolecta*, *P. tricornutum* and *E. huxleyi*. Spline curve fits were added as a visual aid.

The blue head of the ECO BB9 (λ 407 nm, 439 nm, 485 nm) gave much noisier results than the other two. A significant drift had been observed with the sensors from the blue head during the last calibration before ours at the Harbor Branch Institute, which indicated it was perhaps nearing the end of its useful life. These data were removed from the analysis except for *E. Huxleyi* where the results showed consistency with the other wavelengths.

The b_{bp} increased by 50% to 200% during the day, depending on the species and wavelength [Fig. 10]. The σ_{bb} were stable for *T. pseudonana*, *D. tertiolecta* and *P. tricornutum* [Fig. 11], suggesting mostly an influence of biomass (C and cell numbers) on the diurnal variation while changes in the backscattering efficiency per cell have minimal impact. The carbon specific backscattering (b_{bp}^C) [Fig. 11] decreased during the day for *T. pseudonana*, *D. tertiolecta* and *P. tricornutum*. Depending on the storage (lipids, sugars, or other), addition carbon in the cell should modify the index of refraction (or size of the cells) up or down. In this case, it is clear that despite large changes in the carbon per cell, the additional carbon added reduced the backscattering efficiency per unit carbon and did not alter the scattering per cell. This is consistent with the added carbon having little effect on the existing scattering of the cells; the relative decrease in b_{bp}^C being almost equal to the relative increase in carbon per cell (Fig. 4). For *E. huxleyi*, the calcite liths enhance backscattering, so that a higher σ_{bb} was observed. The values were in the range of those observed by Balch et al. [56].

Overall our results for the backscattering ratio ($b_{bp}/b_p (\lambda)$) [Fig. 10(b)] are comparable to those obtained by Whitmire et al. (2010) [57] for *T. pseudonana*, *D. tertiolecta* and *P. tricornutum* (*E. huxleyi* was not studied in Whitmire et al. [56]). Ahn and Bricaud [58]

observed similar values as ours for *D. tertiolecta* for another chlorophyceae, *Dunaliella bioculata*. Their backscattering ratios were, however, lower for *E. huxleyi*, which they grew in nutrient replete medium, while we kept nutrients at lower levels ensuring coccolith production [58]. It is likely that our increased backscattering ratio is due to the presence of coccoliths. Zhou et al. [59] observed a similar backscattering ratio for *T. pseudonana*, but a larger one for *D. tertiolecta*, but their cells were almost twice the size of ours so differences are expected. While the backscattering ratio for *D. tertiolecta* and *E. huxleyi* remained mostly constant throughout the day, it decreased by a factor of about 2 for the diatoms. For all species except *E. huxleyi*, the decreasing carbon specific backscattering coefficient b_{bp}^C ($\text{m}^2 \text{ mg}^{-1}$) with time of day lead to reduced sensitivity of the backscattering coefficient to measuring diel increases in the algal carbon concentration in the water compared with the scattering coefficient (compare the diel increase of b_{bp} in Fig. 10 with b_p Fig. 6). This is particularly obvious with *P. Tricornutum* where b_{bp} hardly increased during the day and b_p increased by a factor of ~2. This could in part arise from the fact that a larger background of small particles is affecting the backscattering and therefore the increase in the backscattering due to algae is hidden, but the cell size distributions do not seem to indicate this.

The chlorophyll-specific backscattering coefficient b_{bp}^{Chl} ($\text{m}^2 \text{ mg}^{-1}$) appeared mostly stable during the day [Fig. 11(b)], except for a daily increase for *E. huxleyi*. Our values of b_{bp}^{Chl} of *E. huxleyi* were higher than those of Ahn and Bricaud [58], because of our increased b_{bp} due to the presence of coccoliths [60]. Their values for a chlorophyceae are in the same range as our values for *D. tertiolecta*.

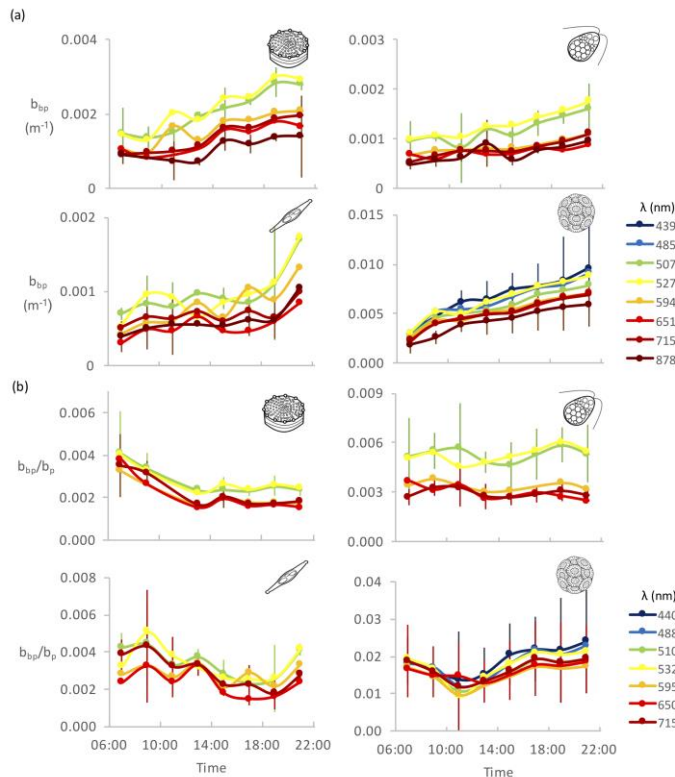


Fig. 10. Diurnal variations of a) the mean particulate backscattering coefficient (b_{bp} , m^{-1}) for the wavelengths indicated and b) the mean backscattering ratio for the wavelengths available from the ECO BB9 and their nearest from the ac-s (in the legend). The standard deviations are only displayed for 440 nm and 715 nm. Results from top to bottom are for: *T. pseudonana*, *D. tertiolecta*, *P. tricornutum* and *E. huxleyi*. Spline curve fits were added as a visual aid.

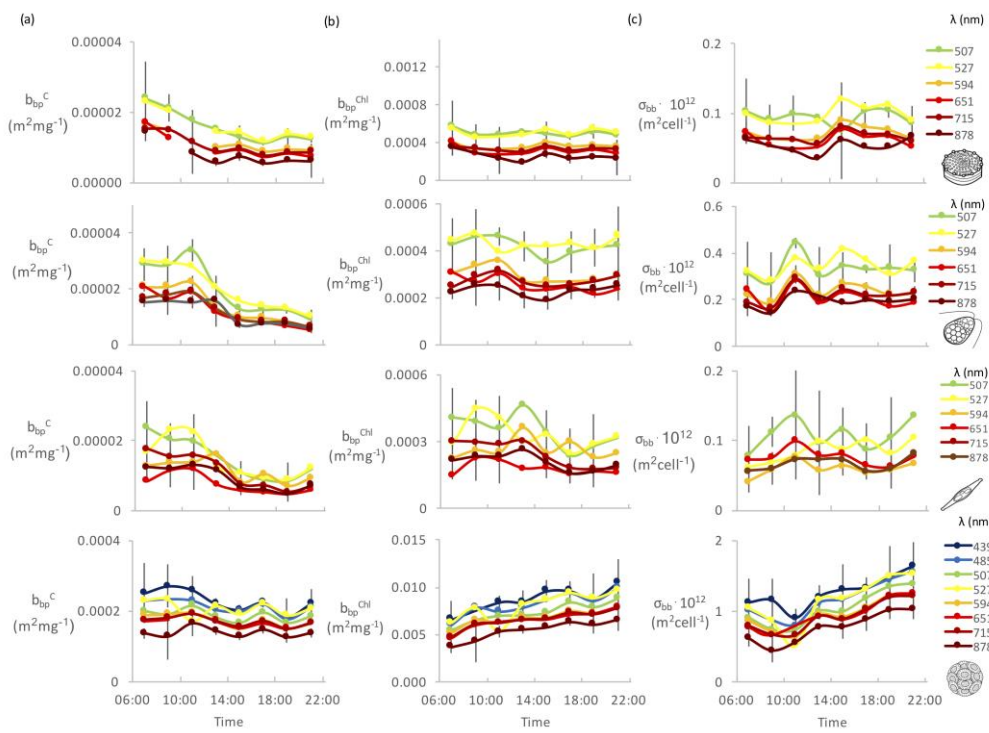


Fig. 11. Diurnal variations of a) the mean C specific particulate backscattering coefficient (b_{bp}^C , $m^2 \text{ mg}^{-1}$), b) Chl specific particulate backscattering coefficient (b_{bp}^{Chl} , $m^2 \text{ mg}^{-1}$) and c) particulate backscattering cross-section ($\sigma_{bb} \cdot 10^{12}$, $m^2 \text{ cell}^{-1}$) for the wavelengths indicated. Standard deviations (error bars) are only displayed for $\lambda = 507$ and 878 nm (439 and 878 nm for *E. huxleyi*). Results from top to bottom are for: *T. pseudonana*, *D. tertiolecta*, *P. tricornutum* and *E. huxleyi*. Spline curve fits were added as a visual aid.

Table 2. Correlation coefficients (r^2) of c_p 716 (m^{-1}) and b_{bp} 715 (m^{-1}) (to avoid the effect of absorption) with cell concentration (n cell, ($\text{Cell} \cdot \text{m}^{-3}$)), carbon content ($\mu\text{g} \cdot \text{L}^{-1}$) and ($\mu\text{g} \cdot \text{cell}^{-1}$), cell diameter (μm) and Chl concentration ($\mu\text{g} \cdot \text{L}^{-1}$) and ($\mu\text{g} \cdot \text{cell}^{-1}$). (Correlation coefficients larger than 0.50 in bold.)

	n cell ($\text{Cell} \cdot \text{m}^{-3}$)	C ($\mu\text{g} \cdot \text{L}^{-1}$)	C ($\mu\text{g} \cdot \text{cell}^{-1}$)	Cell diameter (μm)	Chl ($\mu\text{g} \cdot \text{L}^{-1}$)	Chl ($\mu\text{g} \cdot \text{cell}^{-1}$)	c_p 716 (m^{-1})
<i>T. pseudonana</i>	c_p 716 nm (m^{-1}) 0.60	0.80	0.59	0.29	0.80	0.14	-
	b_{bp} 715 nm (m^{-1}) 0.55	0.68	0.43	0.14	0.72	0.07	0.45
<i>D. tertiolecta</i>	c_p 716 nm (m^{-1}) 0.20	0.81	0.51	0.26	0.81	0.06	-
	b_{bp} 715 nm (m^{-1}) 0.06	0.66	0.60	0.23	0.39	0.08	0.51
<i>P. tricornutum</i>	c_p 716 nm (m^{-1}) 0.59	0.95	0.65	0.51	0.87	0.44	-
	b_{bp} 715 nm (m^{-1}) 0.17	0.09	0.03	0.01	0.16	0.05	0.11
<i>E. huxleyi</i>	c_p 716 nm (m^{-1}) 0.55	0.81	0.29	0.14	0.77	0.03	-
	b_{bp} 715 nm (m^{-1}) 0.54	0.94	0.36	0.16	0.86	0.06	0.79

The particulate backscattering coefficient, b_{bp} , was correlated mostly with C concentration (Table 2), except for *P. tricornutum*, which showed no such correlation. For *E. huxleyi*, the carbon specific backscattering coefficient was stable during the day and b_{bp} was also strongly correlated with C ($\mu\text{g/L}$) ($r^2 = 0.94$, Table 2), more than c_p ($r^2 = 0.81$). For the other species, c_p showed a stronger correlation with biomass indicators (C and Chl per volume) than b_{bp} .

The correlation of b_{bp} with c_p is weaker than observed in nature [37, 61, 62] except for *E. huxleyi*, but these studies were conducted over large gradients and not over a day.

The relative daily changes, Δc_p , Δb_p and Δb_{bp} are all positive [Fig. 12], Δb_{bp} is roughly a factor 2 lower than Δc_p and Δb_p , for all species except for *E. huxleyi*, where Δb_{bp} is higher than Δb_p from midday. The shapes of the variations were similar, except for *E. huxleyi*, where the Δc_p and Δb_p plateaued from midday whereas Δb_{bp} increased throughout the day. Δc_p and Δb_p are much larger than observed in nature, except during bloom conditions when similar values are found [40]. Loisel et al. [39] observed that b_{bp} maxima occurred 3 or 6 hours later than those of c_p . They also noticed relative daily increases were slightly lower for b_{bp} than c_p , but their values were much lower than ours (20–17% for c_p and 13% for b_{bp}), which is expected in nature due to the presence of a higher background of small particles.

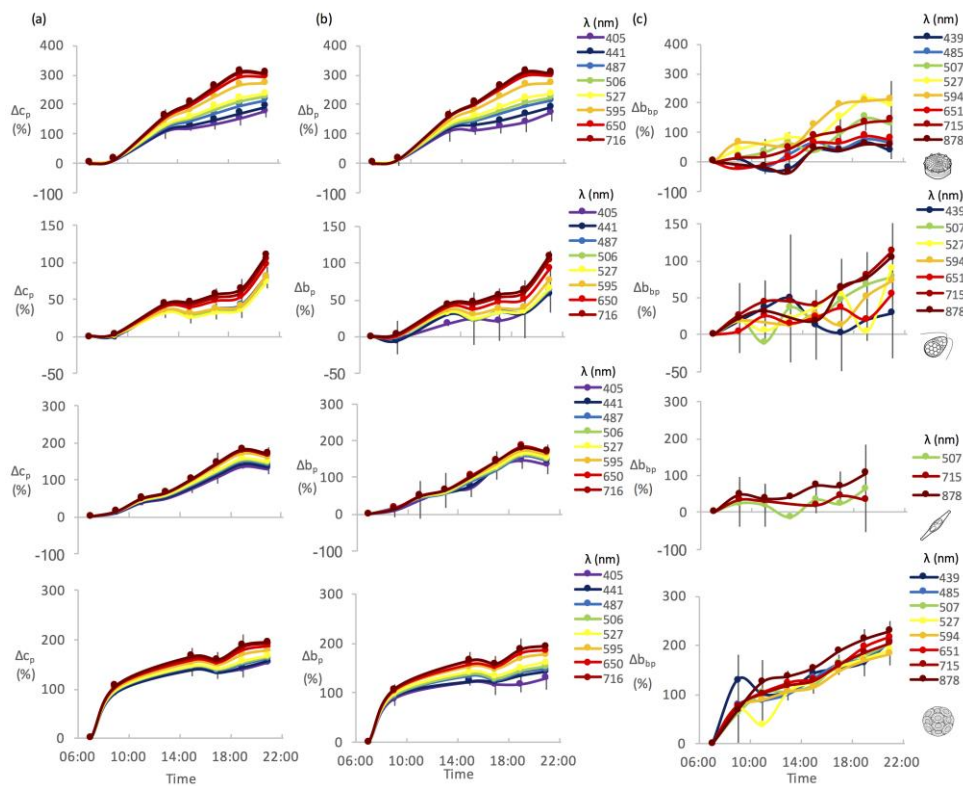


Fig. 12. Diurnal variations of the relative variation from sunrise for a) the particulate attenuation coefficient (Δc_p , %) coefficient b) the particulate scattering coefficient (Δb_p , %) and c) particulate backscattering coefficient (Δb_{bp} , %) for the wavelengths indicated. Standard deviations (error bars) are only displayed for 439 and 878 nm (507 and 878 nm for *P. tricornutum*). Results from top to bottom are for: *T. pseudonana*, *D. tertiolecta*, *P. tricornutum* and *E. huxleyi*. Spline curve fits were added as a visual aid. For *P. tricornutum*, Δb_{bp} was extremely noisy for most wavelengths and thus removed from the analysis.

4. Discussion

4.1. Comparison with the literature

The values and diel changes we obtained for *T. pseudonana* were comparable to what Stramski and Reynold's [21] obtained for the same species, in terms of intracellular carbon and chlorophyll concentration, absorption, scattering and attenuation cross-section. The only notable difference was that we observed a shift in the shape of scattering spectrum. They also did not measure backscattering.

Whitmire et al. [57] studied backscattering properties for many species, including *T. pseudonana*, *D. tertiolecta* and *P. tricornutum*. They obtained values that were similar to ours for the backscattering ratios and cross-sections. Their values for b_{bp}^{Chl} were lower than ours, likely because they used a lower illumination ($100 \mu\text{mol photons m}^2 \text{ s}^{-1}$ vs to $400 \mu\text{mol photons m}^2 \text{ s}^{-1}$ here), leading to a higher intracellular chlorophyll concentration [63].

Durand et al. [23] measured the diel variations of optical properties of a prasinophyte, which cannot be directly compared to our species. They noted similar increases in cell diameter and optical properties, but no the decrease in c_p^C we observed for *D. tertiolecta*.

Ahn and Bricaud [58] studied backscattering properties of various species, including *E. huxleyi*. Their values for backscattering were lower than ours but, as discussed, we used a lower nutrient-content medium to ensure coccolith production that they did not use, so the differences are likely due to the absence of coccoliths in their cultures.

Overall, our results agree with comparable results from the literature. When they do not, the disagreements appear to arise from the different culture conditions.

4.2. Backscattering coefficients measurements

Since we used a single χ value from theory instead of measuring it on our cultures, it can be a source of error in the estimated b_{bp} values. Whitmire et al. [57], Chami et al. [64] and Harmel et al. [65] reported χ values at 120° in cultures varying from approximately 1 to 1.2, which would cause an increase of up to 12% in our b_{bp} values. Tan et al. [66] reported χ values of up to 1.8 for $\beta_p(120^\circ)$ in cultures, but so far, that study is the only reporting such high values, with most studies finding values near 1.1 (see Harmel et al. [65]). The χ values have also been shown to vary between species (Harmel et al. [65], Whitmire et al [57], Tan et al. [66]). This was not considered here when we calculated b_{bp} with a unique χ value. Since χ is only a scaling factor, all b_{bp} values presented here could b_{bp} easily be scaled for any other χ . Since our focus is on the diel changes, a more important question is whether χ could change significantly with time of day for one species. If so, this could alter our conclusion with respect to b_{bp} . Diel measurements of complete volume scattering functions in the future would permit addressing this question. In any case, the relative changes reported for b_{bp} reflect the changes for $\beta_p(124^\circ)$.

We took the outmost care to prevent contamination of our cultures by working in sterile conditions and sterilizing the culture medium. To further avoid the small particles from accumulating in the cultures, we diluted the culture daily with $0.2 \mu\text{m}$ filtered media. However, small detrital particles are always present in cultures. We could not measure particles with a diameter smaller than $2.4 \mu\text{m}$. However, the particle size distributions from the Coulter Counter show an increasing number of particles in the smaller size classes with about 20,000 particles/ml at $2.4 \mu\text{m}$ for all cultures. We subtracted blanks obtained from the Coulter Counter's isotonic dilution solution, such that we know that these particles were present in the cultures. Measurement of blanks (or previous sample) in the measurement container removed the impact of particles present in filtered media used during the measurement. The presence of small particles could enhance measurements of optical properties, particularly backscattering, but it is unlikely that they would influence the diel variations we observed.

4.3. Potential impact on optical observations from space

This study shows that clear diel variations in the particulate backscattering coefficient can be observed on cultures in the laboratory, indicating that phytoplankton are likely responsible for part of the diel variations of b_{bp} observed in the ocean [40]. There is increasing interest in measuring these diel changes as it could be used to estimate the photosynthetic carbon accumulation remotely in the upper ocean in similar way to previous studies with c_p e.g., [12,26,27,36].

However, the fractional contribution of the phytoplankton backscattering to the total particulate backscattering in the ocean remains unclear and is likely dependent on growth conditions. Furthermore, our observation show that while we observed very strong correlation with particulate carbon in some species (*E. huxleyi*), very low correlation was observed with another (*P. tricornutum*); correlation between carbon and c_p were high for all species. Clearly the applicability of our results to in situ and remote sensing observations of b_{bp} diel changes will require further work to understand under which conditions backscattering measurements can be used as a proxy for carbon accumulation in the ocean.

5. Conclusion

We observed diel increases in absorption, beam attenuation and scattering. Our observations with respect to absorption and beam attenuation were consistent with previous studies; the use of the ac-s allowed a greater spectral resolution, but this added limited new insights into the daily changes (though spectral effects do occur). We showed that the carbon-specific beam attenuation coefficient varies during the day and more importantly between species, which has important implications for primary productivity estimations where c_p^C has been assumed to be constant.

The differences between species observed for many of our optical and biological measurements highlights the importance of considering the community structure when studying phytoplankton from optical measurements, especially in presence of coccolithophores, which were often clear outliers.

Our study was the first to study diurnal variations of b_{bp} in cultures, and the observed diurnal increases support the hypothesis that phytoplankton partly drive the diurnal increases in b_{bp} observed in nature. Observations have also shown that the scattering cross section tended to increase during the day along with the carbon specific scattering coefficient. However, the carbon specific backscattering coefficient tended to strongly decrease during the day while the backscattering cross-section remained constant. This result highlights that extreme care should be taken when using diel changes in backscattering as a surrogate for diel changes in scattering, when the latter are to be used to quantify phytoplankton production in the ocean. More specifically, for c_p , the cross section tended to increase while the carbon specific backscattering decreased. What has been learnt from the abundant literature on the diel changes in the scattering coefficient may not be directly applicable to interpretation of the backscattering coefficient.

However, these results overall suggest that particulate backscattering provides a cell-specific measure when phytoplankton are a significant source of backscattering.

This study also reaffirms that the observation of diurnal variations of optical properties of phytoplankton can give us valuable insights in understanding the biological and bio-optical processes that occur in the ocean. Modeling work will be necessary to tease apart the possible origins of these differences and could help with the interpretation of diurnal patterns in the backscattering coefficient as potentially observed from ocean color satellite remote sensing.

Funding

FRQNT; NSERC; Canada Research Chair program.

Acknowledgments

We thank Gabriel Diab, Pascale Roy, Tara Tapics, Simon Meilleur-Lacasse, Jennifer Marie-Rose Vandenhecke, Patrick Cliche, Dominic Bélanger, Dominique Marie and Marieke Beaulieu for their precious help before and during the experiments. We are indebted to Emmanuel Boss for loaning the ac-s and ECO-BB9 used and comments, Marie-Hélène Laprise for sharing the flow cytometer and Zbigniew Kolber for loaning the FRRF fluorimeter. Thanks to Darius Stramski, Mike Twardowski and Malika Kheireddine and an anonymous reviewer for their valuable comments on this work.